Electronic Supplementary Material (ESI) for Journal of Materials Chemistry A.

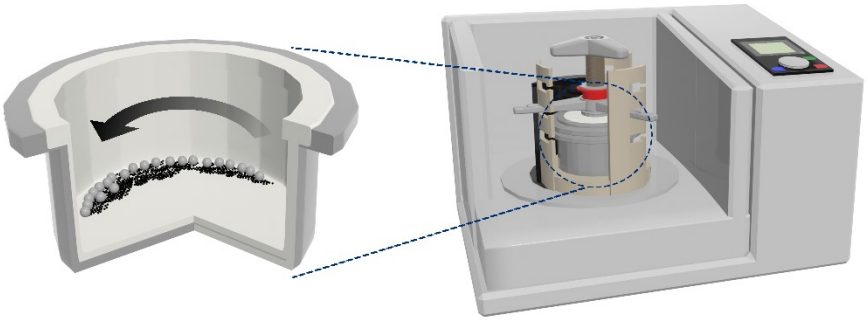

Fig. S1. Illustration of the super-mill process.

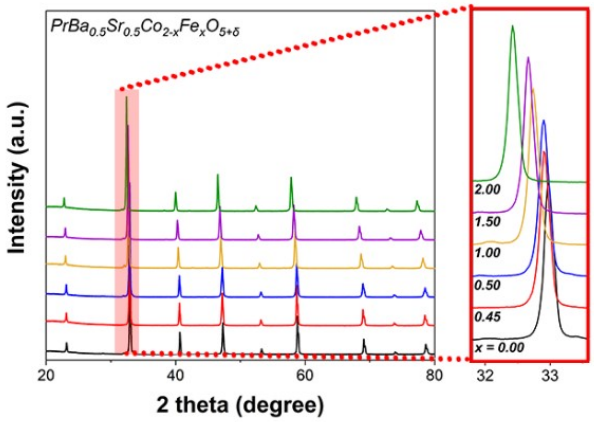

Fig. S2. X-ray diffraction patterns of PBSCF catalysts.

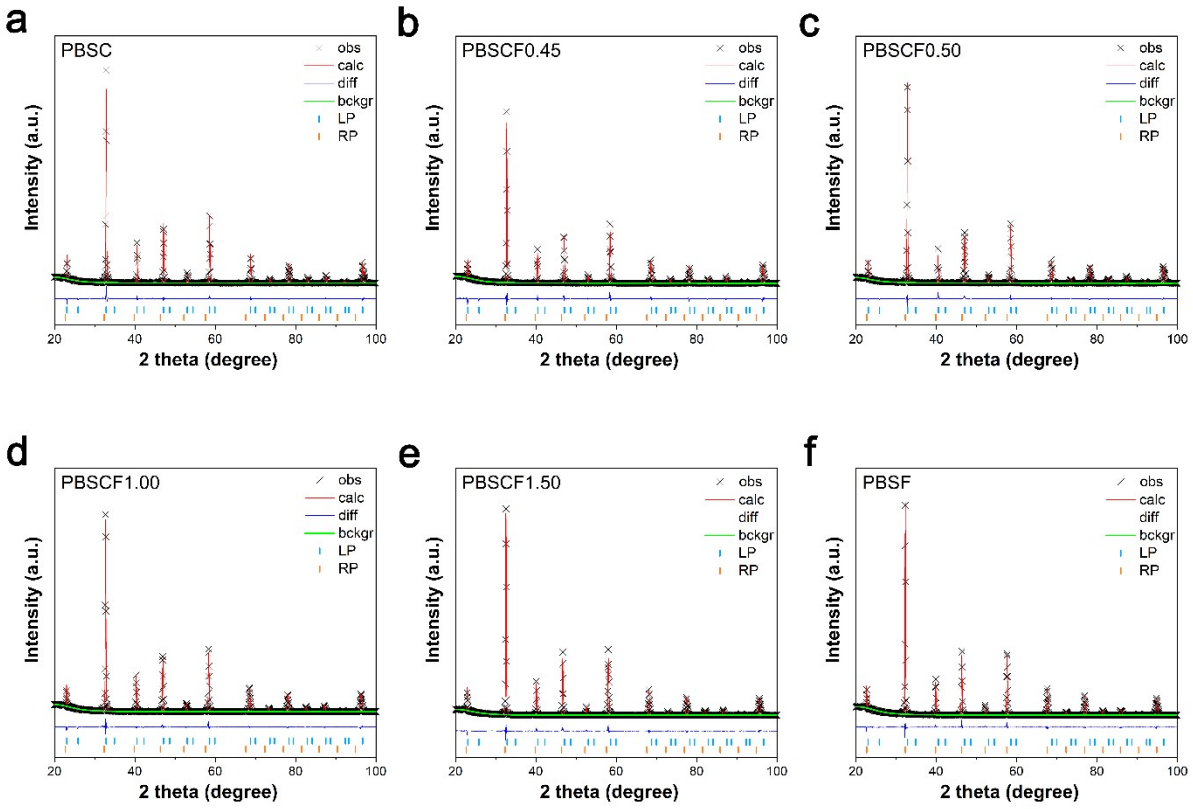

Fig. S3. Rietveld refinement of XRD patterns of PBSCF. The lattice parameter is shown in Table S2.

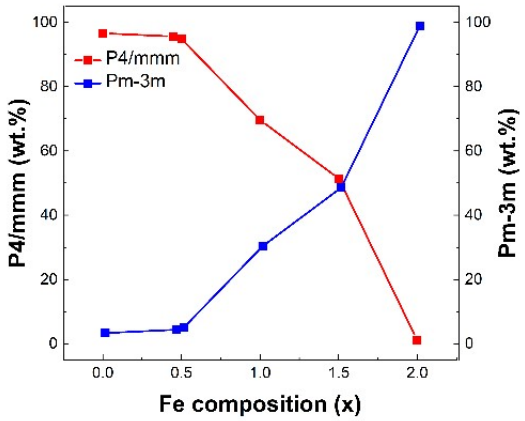

Fig. S4. The ratio of RP (*Pm-3m*) and LP (*P4/mmm*) was calculated by the results of the Rietveld refined XRD pattern of PBSCF.

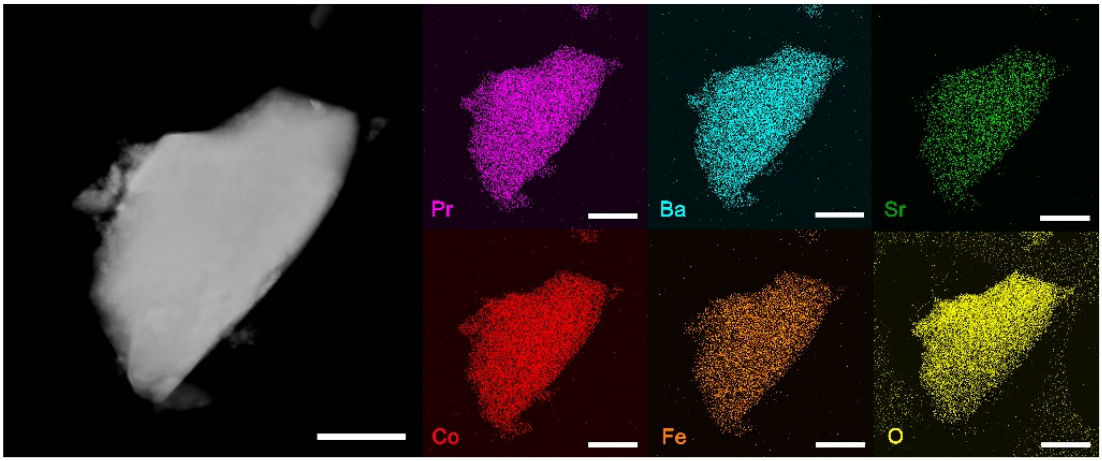

Fig. S5. Dark-filed scanning transmission electron microscope (STEM) image and STEM-EDS element mapping of PBSCF0.45 (Scale bar: 100 nm).

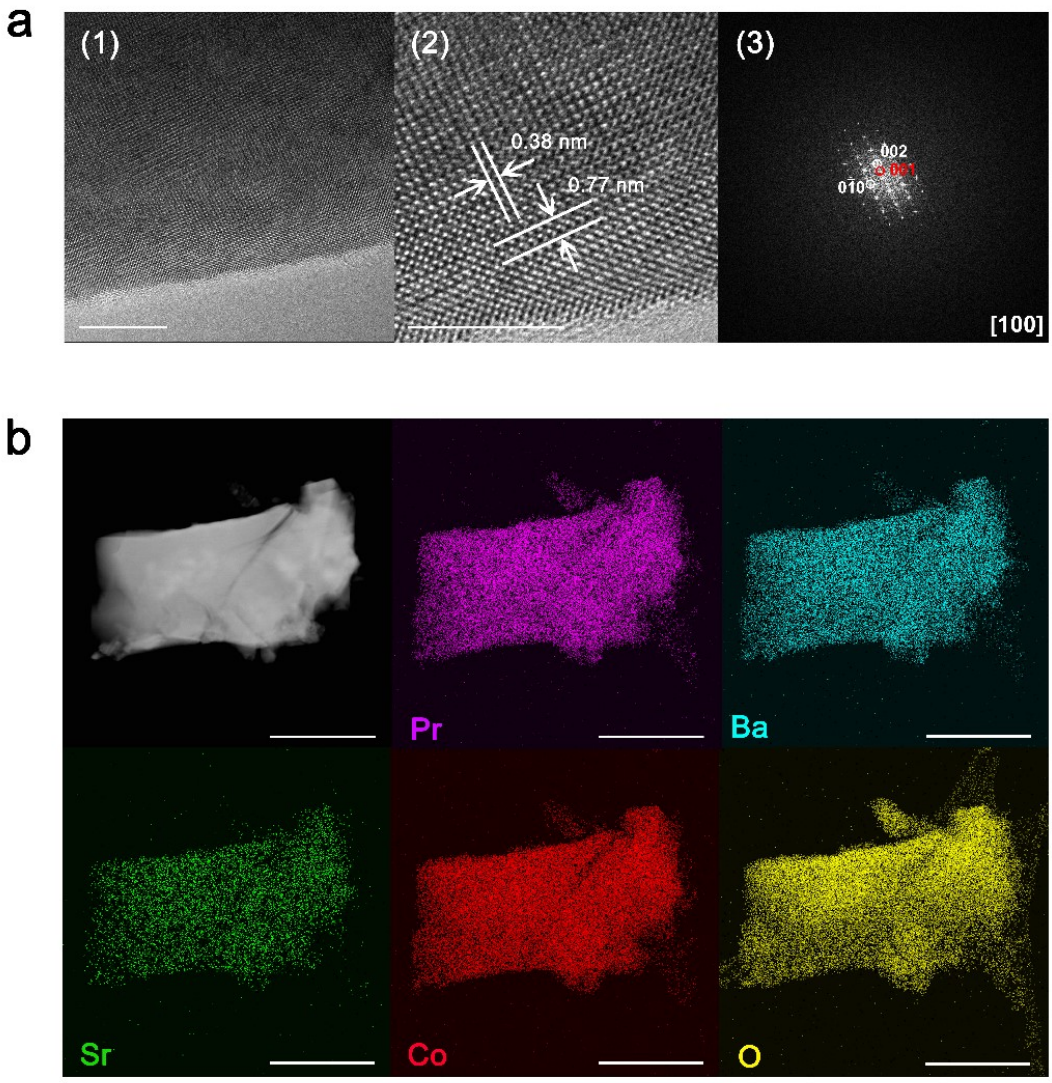

Fig. S6. a) HR-TEM image of PBSC, and (3) corresponding FFT pattern (Scale bar: (1) 10 nm and (2) 5 nm). b) STEM image and STEM-EDS element mapping of PBSC (Scale bar: 500 nm).

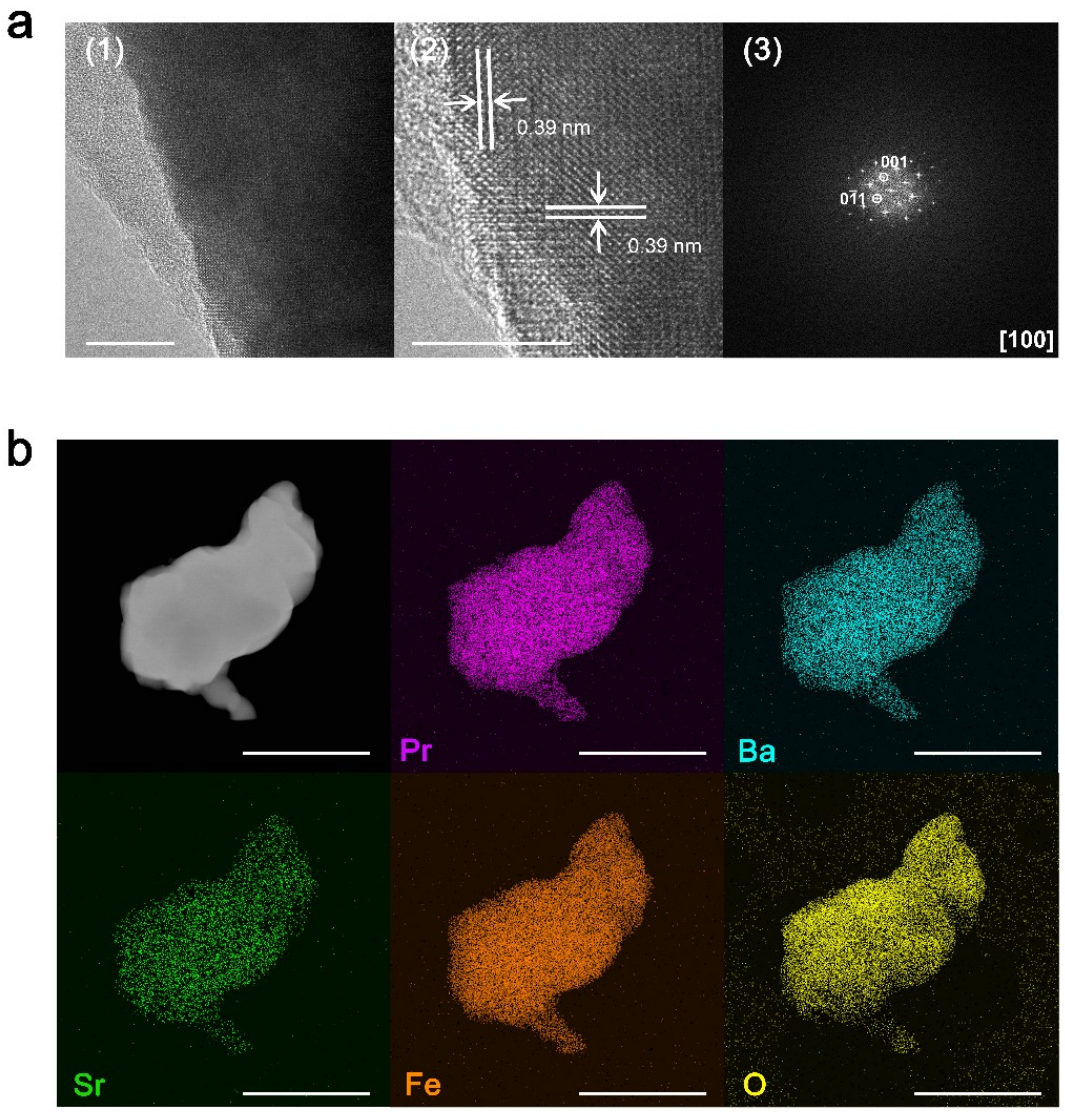

Fig. S7. a) HR-TEM image of PBSF, and (3) corresponding FFT pattern (Scale bar: (1) 10 nm and (2) 5 nm). b) STEM image and STEM-EDS element mapping of PBSF (Scale bar: 1 μm).

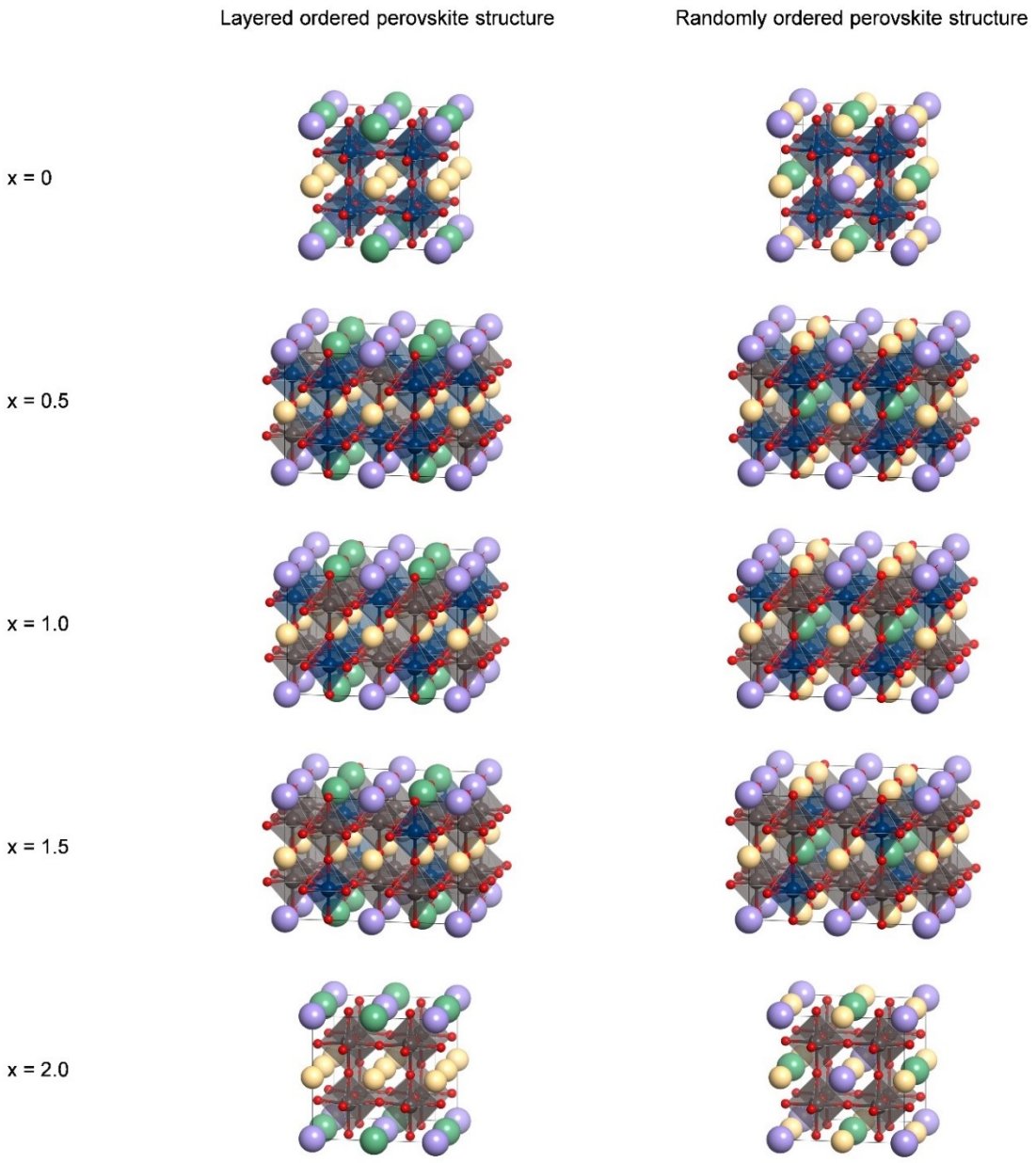

Fig. S8. Optimized structures of layered and randomly ordered $PrBa_{0.5}Sr_{0.5}Co_{2-x}Fe_xO_6$ (x = 0, 0.5, 1.0, 1.5, and 2.0). Praseodymium, barium, strontium, cobalt, iron, and oxygen are yellow, green, purple, blue, brown, and red, respectively.

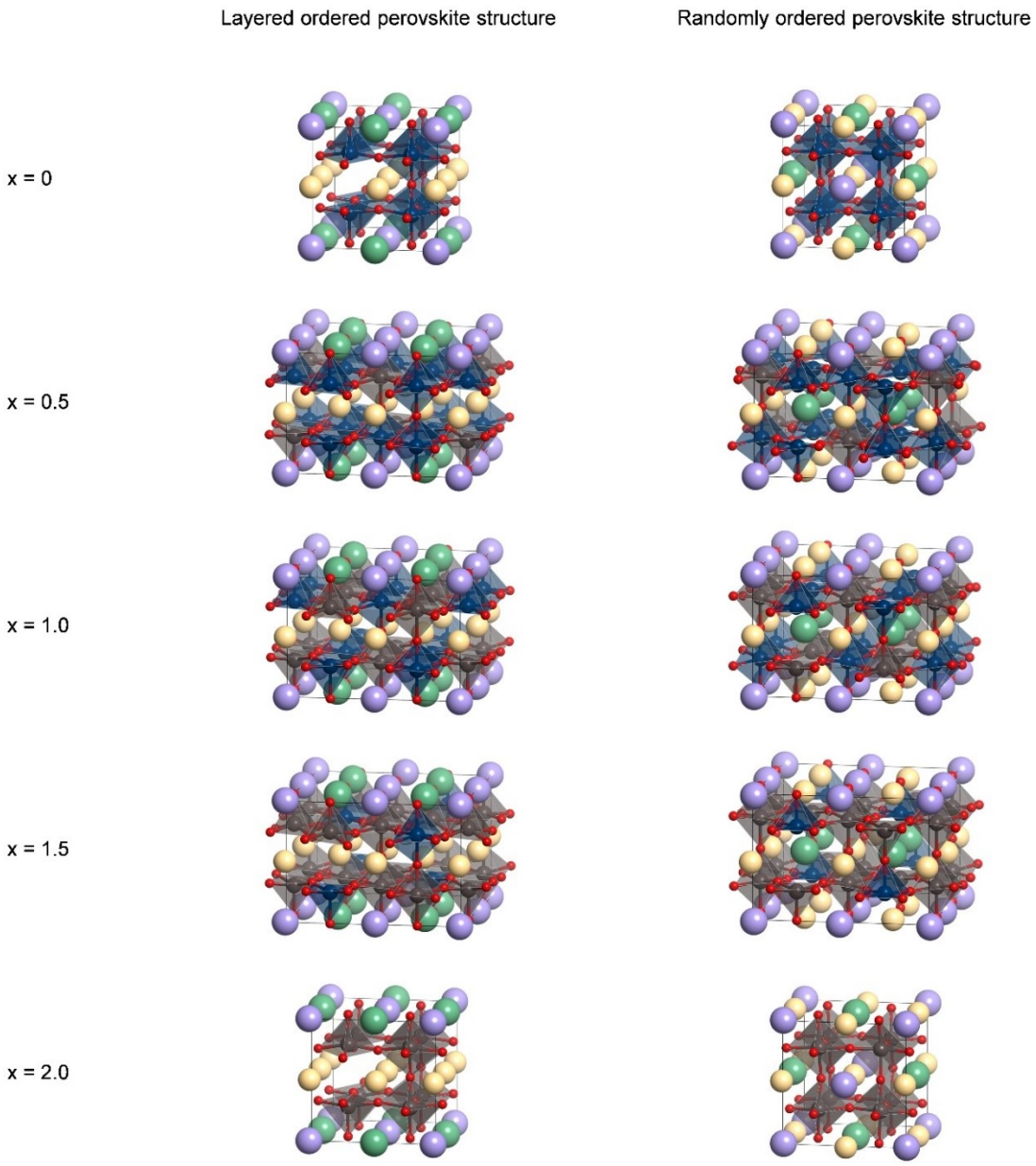

Fig. S9. Optimized structures of layered and randomly ordered $PrBa_{0.5}Sr_{0.5}Co_{2-x}Fe_xO_{5.5}$ (x = 0, 0.5, 1.0, 1.5, and 2.0). Praseodymium, barium, strontium, cobalt, iron and oxygen are yellow, green, purple, blue, brown and red, respectively.

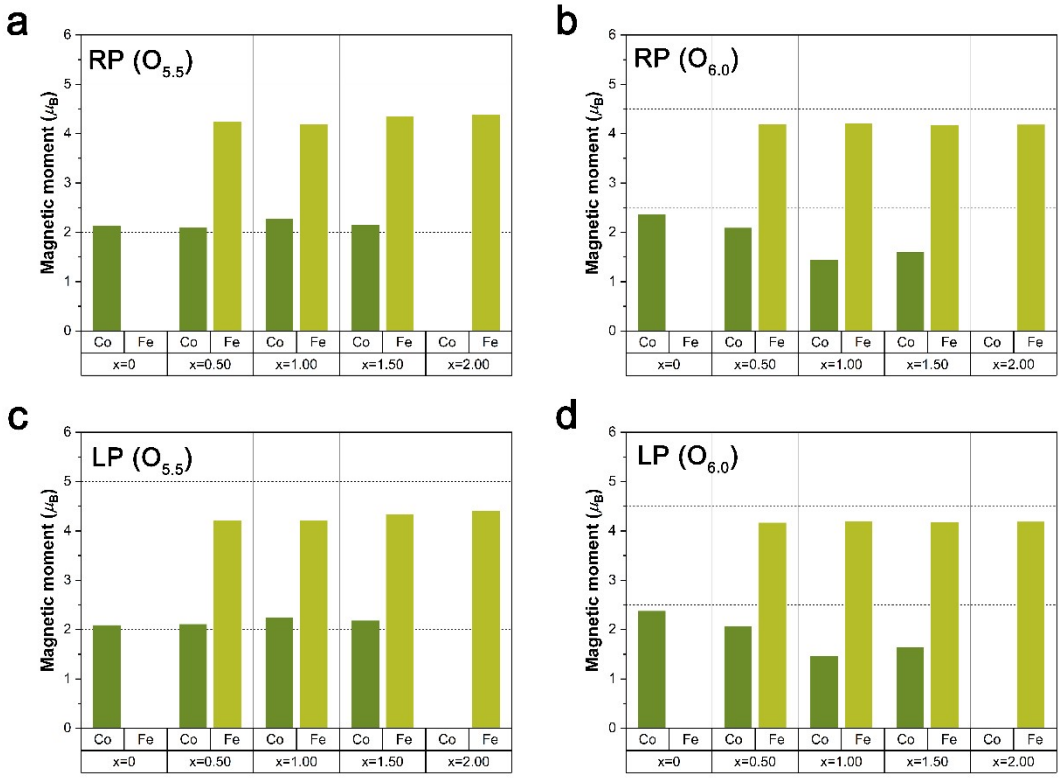

Fig. S10. The average magnetic moment of Co and Fe for PBSCF catalysts of RP structure at (a) δ = 0.5 and (b) δ = 0.0. The average magnetic moment of Co and Fe for PBSCF catalysts of LP structure at (c) δ = 0.5 and (d) δ = 0.0.

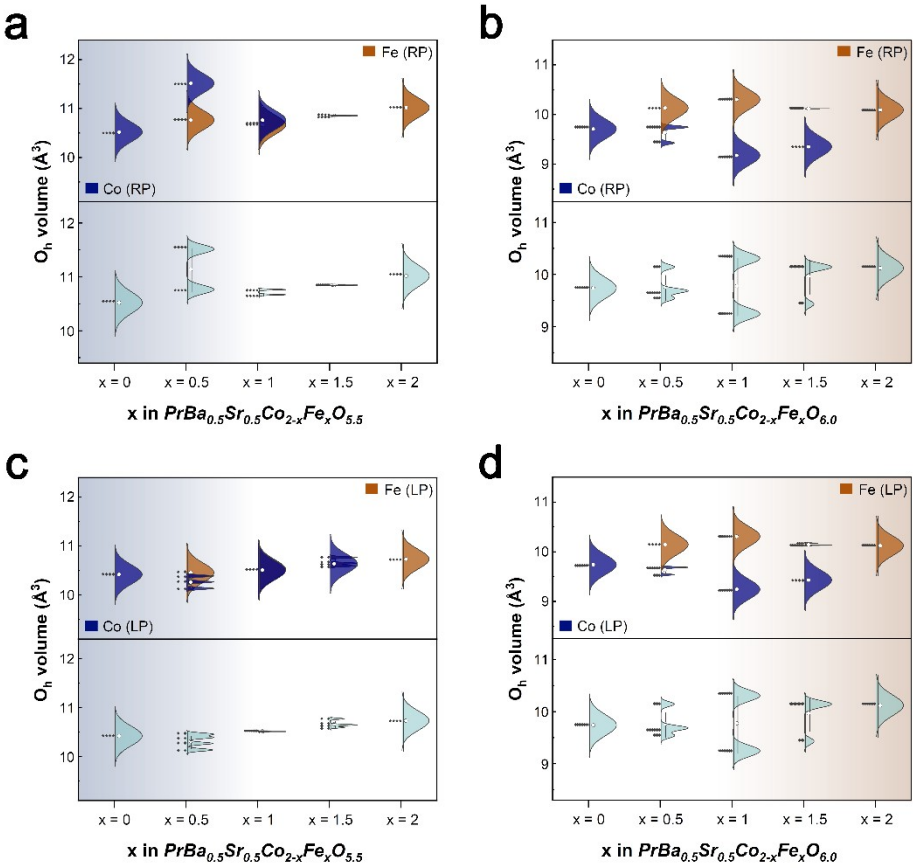

Fig. S11. Distribution of CoO_6 and FeO_6 octahedron volume for PBSCF catalysts of RP structure at (a) $\delta = 0.5$ and (b) $\delta = 0.0$. Distribution of CoO_6 and FeO_6 octahedron volume for PBSCF catalysts of LP structure at (c) $\delta = 0.5$ and (d) $\delta = 0.0$.

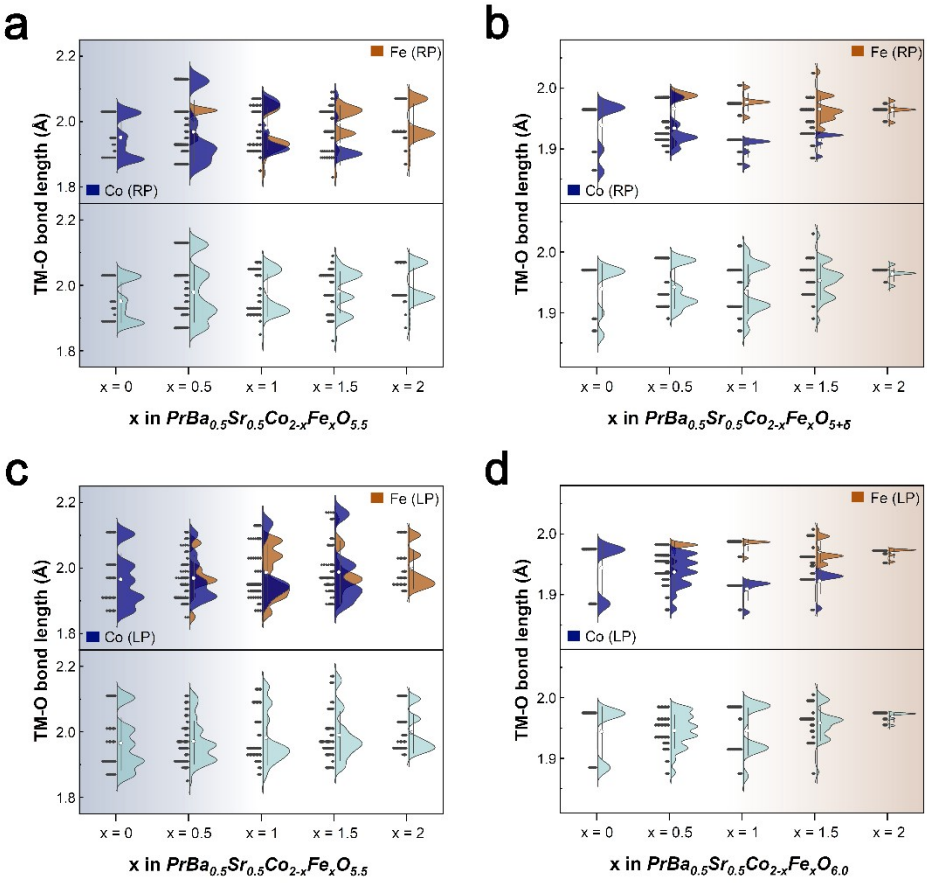

Fig. S12. Co-O and Fe-O bond length for PBSCF catalysts of RP structure at (a) δ = 0.5 and (b) δ = 0.0. Co-O and Fe-O bond length for PBSCF catalysts of LP structure at (c) δ = 0.5 and (d) δ = 0.0.

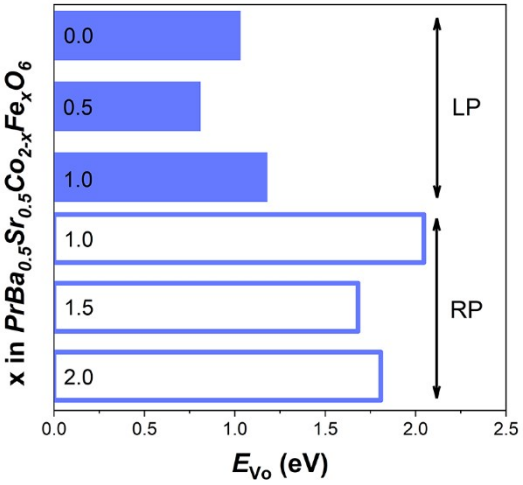

Fig. S13. Oxygen vacancy formation energy (E_{Vo}) of major phase for each Fe content (i.e., LP structure at x < 1 and RP structure at x > 1, $PrBa_{0.5}Sr_{0.5}Co_{2-x}Fe_xO_6$).

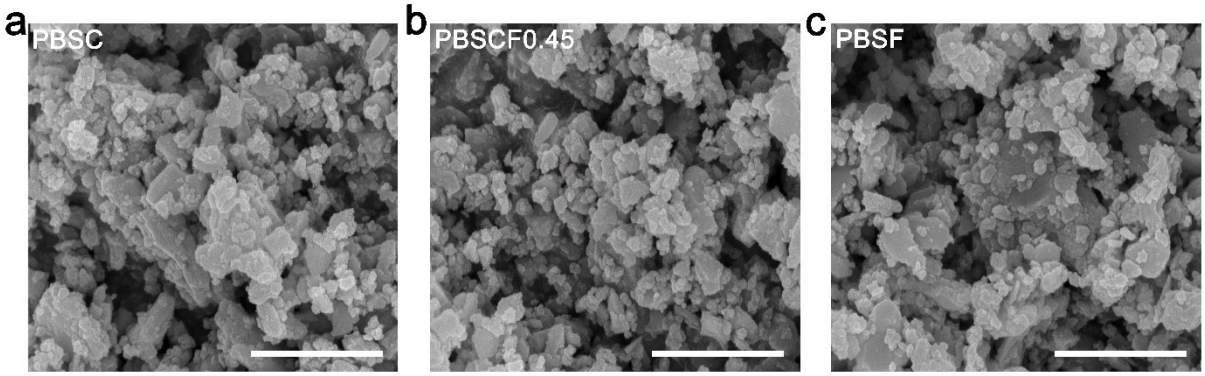

Fig. S14. SEM image of (a) PBSC, (b) PBSCF0.45 and (c) PBSF (Scale bar: 1 μm).

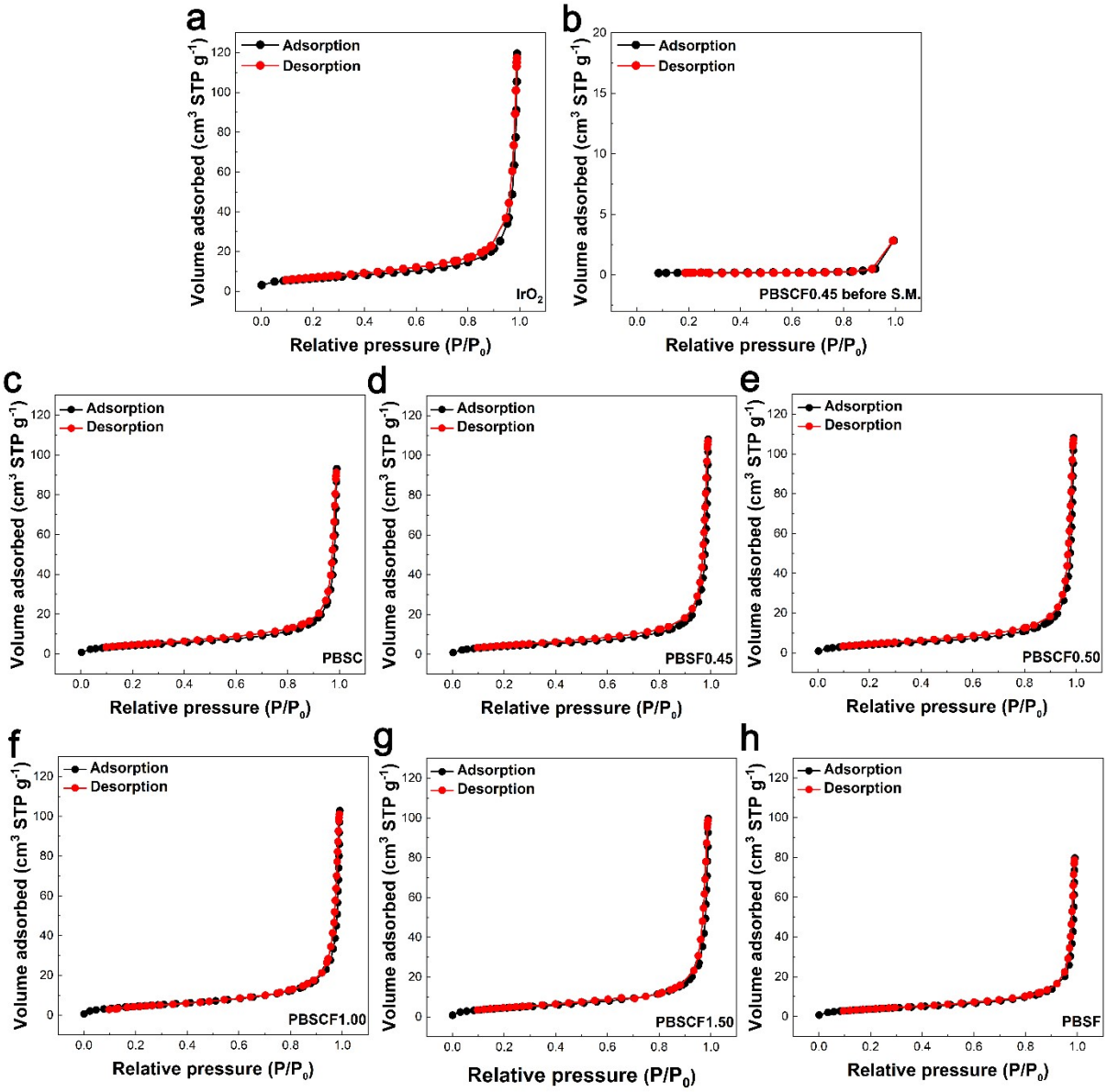

Fig. S15. N_2 adsorption/desorption isotherms of a) IrO_2, b) PBSCF0.45 before S.M. and c-h) PBSCF catalysts. BrunauerEmmett-Teller (BET) specific surface areas and pore size distribution calculated by the results of N_2 adsorption/desorption isotherms are shown in Table S3.

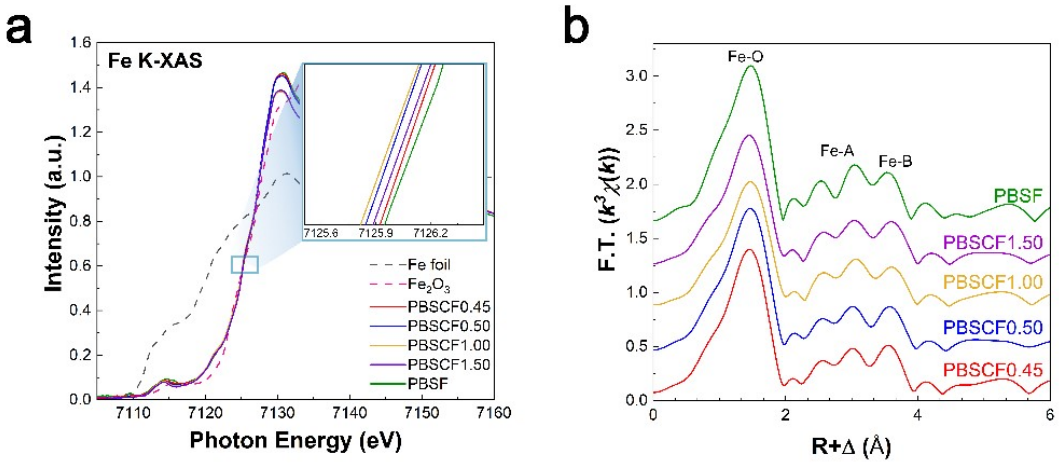

Fig. S16. a) Normalized Fe K-edge XANES of PBSCF catalysts. The inset shows the photon energy at an intensity of 0.8. b) Fourier transforms of Fe K-edge k^3-weighted EXAFS for PBSCF catalysts.

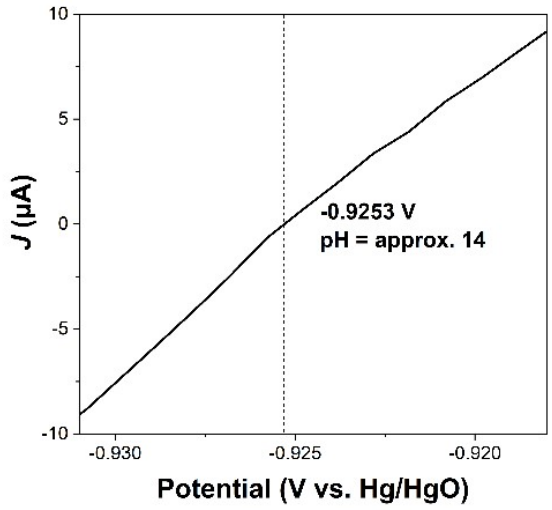

Fig. S17. RHE calibration. For the RHE calibration of the Hg/HgO reference electrode, the potential was swept at 1 mV s^{-1} in H_2 saturated 1 M KOH. Pt wire was used as the working and counter electrode.

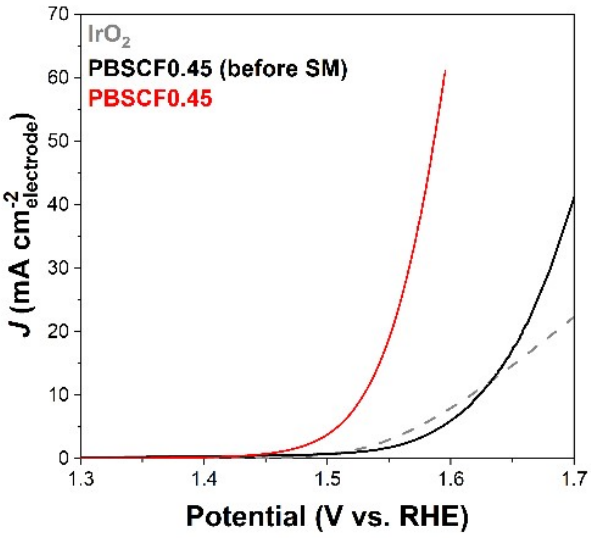

Fig. S18. CV curves of PBSCF, PBSCF before SM, and IrO_2 in N_2-saturated 1M KOH solution.

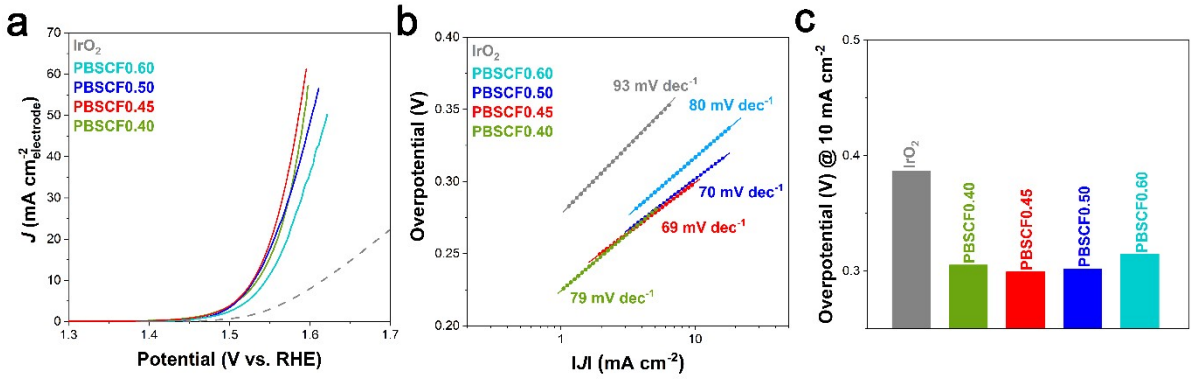

Fig. S19. CV curves of PBSCF0.40, PBSCF0.45, PBSCF0.50, and PBSCF0.60 in N_2-saturated 1M KOH solution.

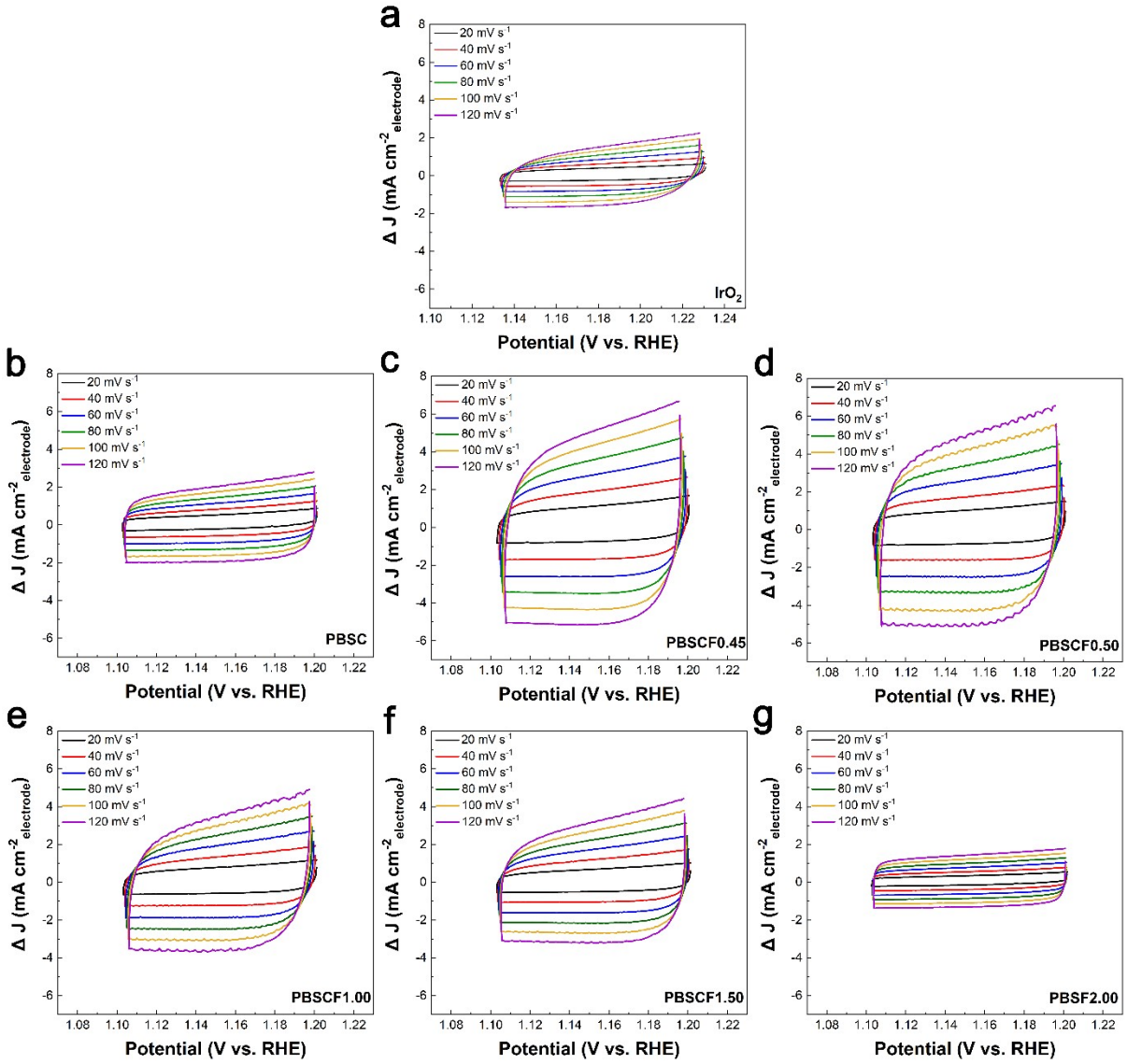

Fig. S20. Electrochemical CV scans were recorded for a) IrO_2 and b-g) PBSCF catalysts at different potential scanning rates. Scan rates are 20, 40, 60, 80, 100, and 120 mV s^{-1}. The selected potential range where no faradic current was observed at 1.12 to 1.24 V *vs.* RHE.

Table S1. Chemical compositions and abbreviations of each sample.

Compound	Abbreviations
$PrBa_{0.5}Sr_{0.5}Co_{2-x}Fe_xO_{5+\delta}$	PBSCF
$PrBa_{0.5}Sr_{0.5}Co_{2.00}O_{5+\delta}$	PBSC
$PrBa_{0.5}Sr_{0.5}Co_{1.55}Fe_{0.45}O_{5+\delta}$	PBSCF0.45
$PrBa_{0.5}Sr_{0.5}Co_{1.50}Fe_{0.50}O_{5+\delta}$	PBSCF0.50
$PrBa_{0.5}Sr_{0.5}Co_{1.00}Fe_{1.00}O_{5+\delta}$	PBSCF1.00
$PrBa_{0.5}Sr_{0.5}Co_{0.50}Fe_{1.50}O_{5+\delta}$	PBSCF1.50
$PrBa_{0.5}Sr_{0.5}Fe_{2.00}O_{5+\delta}$	PBSF

Table S2. Lattice information of PBSCF catalysts determined in Rietveld refinement.

Sample	PBSC	PBSCF0.45	PBSCF0.50	PBSCF1.00	PBSCF1.50	PBSF
Pm-3m (wt.%)	3.36	4.4	5.07	30.34	48.6	98.9
a (Å)	3.86	3.865	3.866	3.872	3.894	3.915
b (Å)	-	-	-	-	-	-
c (Å)	-	-	-	-	-	-
V ($Å^3$)	57.51	57.75	57.77	58.05	59.04	59.9
*P*4/*mmm* (wt.%)	96.64	95.6	94.93	69.66	51.4	1.1
a (Å)	3.861	3.864	3.863	3.875	3.893	3.915
b (Å)	-	-	-	-	-	-
c (Å)	7.715	7.738	7.744	7.766	7.795	7.825
V ($Å^3$)	115	115.54	115.57	116.63	118.12	119.96
R_{wp}	6.44	4.71	4.79	5.33	6.64	5.45
R_p	4.15	3.1	3.43	3.27	3.93	3.52

Table S3. Brunauer-Emmett-Teller (BET) surface area analysis results of the IrO_2 benchmark catalyst and PBSCF catalysts.

Sample	$a_{s,BET}$ ($m^2\ g^{-1}$)	Total pore volume ($cm^3\ g^{-1}$)	Mean pore diameter (nm)
IrO_2	22.18	0.1763	31.80
PBSC	17.51	0.0467	10.67
PBSCF0.45	18.65	0.1968	40.92
PBSCF0.50	18.39	0.1764	37.83
PBSCF1.00	17.72	0.1588	35.84
PBSCF1.50	17.79	0.1565	35.18
PBSF	17.26	0.0399	9.25
PBSCF0.45 (before SM)	1.51	0.0071	18.635

Table S4. Comparison of electrocatalyst performance of IrO_2 benchmark catalyst and PBSCF catalysts for OER. η is the overpotential (V) at 10 mA cm^{-2} from 1.23 V vs RHE, C_{dl} is the double layer capacitance at 1.18 vs. RHE with different scan rates and R_{ct} is the charge-transfer resistance at 1.48 V vs RHE.

Sample	η (V)	Tafel slope (mV dec^{-1})	C_{dl} (mF cm^{-2})	R_{ct} (Ω cm^2)
IrO_2	0.387	99	12.19	33.47
PBSC	0.356	98	16.35	26.73
PBSCF0.45	0.299	69	42.23	4.53
PBSCF0.50	0.302	70	41.52	4.60
PBSCF1.00	0.333	84	28.99	13.04
PBSCF1.50	0.344	93	26.25	15.87
PBSF	0.373	124	15.95	29.26

Table S5. Survey of overpotential at 10 mA cm^{-2} current density for OER electrocatalyst in 1M KOH electrolyte.

Catalyst	Current density (mA cm^{-2})	Overpotential (V)	Electrolyte	Ref.
PBSCF0.45	10	0.29	1 M KOH	This work
IrO_2	10	0.38	1 M KOH	This work
$La_{0.8}Sr_{0.2}Co_{0.6}Ni_{0.4}O_{3-\delta}$	10	0.29	1 M KOH	J. Alloys Compd. 831, 154728 (2020)
$SrFe_{0.57}Co_{0.27}Mo_{0.16}O_{2.99}$ /$Sr_2Fe_{0.85}Co_{0.17}Mo_{0.56}Ni_{0.42}O_6$	10	0.29	1 M KOH	ChemSusChem. 13, 11, 3045-3052 (2020)
$SrCo_{0.2}Fe_{0.2}W_{0.4}O_{3-\delta}$	10	0.30	1 M KOH	J. Mater. Chem. A. 6, 9854-9859 (2018)
$LaFeNiO_3$ Nanorods	10	0.30	1 M KOH	Angew. Chem. Int. Ed. 131, 18, 2338-2342 (2019)
$Ba_{0.9}Sr_{0.1}Co_{0.8}Fe_{0.1}Ir_{0.1}O_{3-\delta}$	10	0.30	1 M KOH	ACS Appl. Energy Mater. 3, 7, 7149-7158 (2020)
$SrCo_{0.4}Fe_{0.2}W_{0.4}O_{3-\delta}$	10	0.30	1 M KOH	J. Mater. Chem. A. 6, 9854-9859 (2018)
$LaCo_{0.8}V_{0.2}O_3$	10	0.31	1 M KOH	ChemSusChem. 13, 10, 2671-2676 (2020)
$SmBaCo_{1.5}Mn_{0.5}O_{5+\delta}$	10	0.31	1 M KOH	Crystals. 3, 10, 205 (2020)
$La_{0.4}Sr_{0.6}Ni_{0.5}Fe_{0.5}O_3$	10	0.32	1 M KOH	Front. Chem. 7, 224 (2019)
$BaCo_{0.4}Fe_{0.4}Zr_{0.1}Y_{0.1}O_{3-\delta}$	10	0.32	1 M KOH	J. Mater. Chem. A, 6, 17288-17296 (2018)
$SrCo_{0.5}Fe_{0.5}O_{3-\delta}$-800	10	0.327	1 M KOH	J. Mater. Chem. A, 8, 6480-6486 (2020)
$Sr_3FeCoO_{7-\delta}$	10	0.343	1 M KOH	J. Mater. Chem. A, 6, 14240-14245 (2018)
Fe-$LaNiO_3$	10	0.35	1 M KOH	Research, 15, 6961578, (2020)
CQDs@BSCF-NFs	10	0.35	1 M KOH	Appl. Catal. B, 257, 117919 (2019)
$La_{0.5}(Ba_{0.4}Sr_{0.4}Ca_{0.2})_{0.5}Co_{0.8}Fe_{0.2}O_{3-\delta}$	10	0.35	1 M KOH	Adv. Energy Mater. 7, 1700666 (2017)
$SrCo_{0.8}Fe_{0.5-x}O_{3-\delta}/Fe_xO_y$	10	0.352	1 M KOH	ACS Appl. Mater. Interfaces, 13, 15, 17439–17449 (2021)
La_2NiMnO_6	10	0.37	1 M KOH	J. Am. Chem. Soc., 140, 36, 11165-11169 (2018)

$SrNb_{0.1}Co_{0.7}Fe_{0.2}O_{3-\delta}$ nanorods	10	0.39	1 M KOH	Adv. Energy Mater. 7, 1602122 (2017)
$LaCo_{0.8}Fe_{0.2}O_3$	10	0.39	1 M KOH	ChemElectroChem, 7, 12, 2564-2574 (2020)
BPMC/NCNT-20	10	0.39	1 M KOH	Chem. Commun. 56, 8277-8280 (2020)
$LaNiO_3$	10	0.42	1 M KOH	Research, 15, 6961578, (2020)
$LaCoO_3$	10	0.44	1 M KOH	J. Electroanal. Chem. 809, 22-30 (2018)
10 nm films-BSCF-Ni	10	0.46	1 M KOH	Sci. Adv. 3, 1603206 (2017)
La_2NiFeO_6	10	0.46	1 M KOH	Research, 15, 6961578, (2020)
$BaPrMn_{1.75}Co_{0.25}O_{5+\delta}$	10	0.49	1 M KOH	Chem. Commun. 56, 8277-8280 (2020)
$SrNb_{0.1}Co_{0.7}Fe_{0.2}O_{3-\delta}$	10	0.50	1 M KOH	Adv. Energy Mater. 7, 1602122 (2017)
BSCF thin films	10	0.57	1 M KOH	Electrochim. Acta, 218, 156-162 (2016)
$PrBaCo_2O_{5+\delta}$	10	0.77	1 M KOH	ACS Catal. 7, 10, 7029–7037 (2017)